A Gastropod Toxin Selectively Slows Early Transitions in the Shaker K Channel's Activation Pathway

Jon T. Sack,[1,2] Richard W. Aldrich,[2] and William F. Gilly[1]

[1]Hopkins Marine Station of Stanford University, Department of Biological Sciences, Pacific Grove, CA 93950
[2]Department of Molecular and Cellular Physiology, Howard Hughes Medical Institute, Stanford University School of Medicine, Stanford, CA 94305

ABSTRACT A toxin from a marine gastropod's defensive mucus, a disulfide-linked dimer of 6-bromo-2-mercaptotryptamine (BrMT), was found to inhibit voltage-gated potassium channels by a novel mechanism. Voltage-clamp experiments with Shaker K channels reveal that externally applied BrMT slows channel opening but not closing. BrMT slows K channel activation in a graded fashion: channels activate progressively slower as the concentration of BrMT is increased. Analysis of single-channel activity indicates that once a channel opens, the unitary conductance and bursting behavior are essentially normal in BrMT. Paralleling its effects against channel opening, BrMT greatly slows the kinetics of ON, but not OFF, gating currents. BrMT was found to slow early activation transitions but not the final opening transition of the Shaker ILT mutant, and can be used to pharmacologically distinguish early from late gating steps. This novel toxin thus inhibits activation of Shaker K channels by specifically slowing early movement of their voltage sensors, thereby hindering channel opening. A model of BrMT action is developed that suggests BrMT rapidly binds to and stabilizes resting channel conformations.

KEY WORDS: Shaker • Kv • gating • potassium channel • neurotoxin

INTRODUCTION

The activation path of Shaker (ShBΔ) potassium channels consists of many voltage-dependent transitions between closed states, culminating in a single open state (Hoshi et al., 1994; Schoppa and Sigworth, 1998a). Transitions early in the activation pathway determine the characteristic delay and sigmoidal time course with which K current (I_K) rises after a positive voltage step (Zagotta et al., 1994a; Schoppa and Sigworth, 1998c; Ledwell and Aldrich, 1999). These early voltage-dependent transitions are thought to occur independently in each of the channel's four α-subunits (Zagotta et al., 1994a; Schoppa and Sigworth, 1998c). Early transitions also determine the time course of ON gating current (I_gON) (Bezanilla et al., 1994; Zagotta et al., 1994a; Schoppa and Sigworth, 1998c), which reflects movements of the channel's voltage sensors.

After these early transitions, the four subunits appear to undergo one or more highly cooperative steps, resulting in the channel opening to potassium permeation. These late steps involve only 10–20% of the total gating charge (Schoppa and Sigworth, 1998c; Ledwell and Aldrich, 1999) and normally occur so quickly that they have only minor effects on the time course of I_gON or I_K activation. When channels deactivate, these late steps are first in the reverse pathway. When the channels deactivate, these late steps are rate limiting for both I_gOFF and I_K "tail" currents as the channels close (Zagotta et al., 1994a; Schoppa and Sigworth, 1998c).

Later activation steps are kinetically adjacent to the open state, and much has been learned about them by studying the behavior of macroscopic and single-channel I_K. This experimental advantage has aided identification of specific mutations that separate the final cooperative opening step from earlier gating transitions (Baker et al., 1998; Schoppa and Sigworth, 1998b; Smith-Maxwell et al., 1998b; Ledwell and Aldrich, 1999; Mannuzzu and Isacoff, 2000). The dynamics of states later in the activation pathway have also been probed with a variety of compounds that preferentially block open channels (Armstrong, 1966, 1971; Choi et al., 1993; Holmgren et al., 1997; Brock et al., 2001; Melishchuk and Armstrong, 2001). One gating modifier, 4-aminopyridine, has been reported to inhibit only the final transition to the open state, revealing the energetics of that final opening step (Armstrong and Loboda, 2001; Loboda and Armstrong, 2001).

In contrast, early gating transitions have been far more difficult to study. Although gating currents pro-

Address correspondence to William F. Gilly, Hopkins Marine Station of Stanford University, 120 Ocean View Boulevard, Pacific Grove, CA 93950. Fax: (831) 375-0793; email: lignje@stanford.edu

Abbreviations used in this paper: BrMT, 6-bromo-2-mercaptotryptamine; HEPES, N-2-hydroxyethylpiperazine-N′-2-ethanesulfonic acid; ShBΔ, Shaker B(Δ6−46); NMG, N-methyl-D-glucamine; TCEP, tris-carboxyethylphosphine.

J. Gen. Physiol. © The Rockefeller University Press • 0022-1295/2004/06/685/12 $8.00
Volume 123 June 2004 685–696
http://www.jgp.org/cgi/doi/10.1085/jgp.200409047

vide an informative signal about these transitions, details about individual early steps have been difficult to extract. Pharmacological approaches using ligands that specifically alter early gating steps would be of great value in studying early transitions, but few agents of this sort are presently available.

Recently, we identified the disulfide-linked dimer of 6-bromo-2-mercaptotryptamine (BrMT) as a novel toxin that slows K-channel activation gating (Kelley et al., 2003).

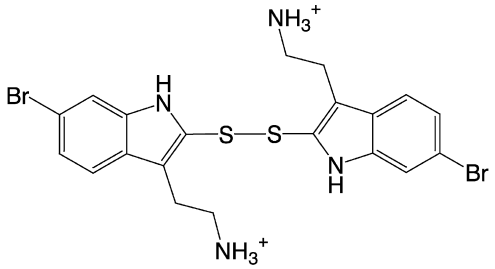

BrMT

BrMT was isolated from a marine snail (*Calliostoma canaliculatum*) and is a component of the gastropod's defensive mucus. This toxin has a unique pharmacology, as it slows activation of Kv1 (Shaker-type), Kv4, and EAG channels, but not Kv2 or Kv3 channels (Kelley et al., 2003).

In this paper we determine that BrMT inhibits activation of Shaker K channels by a novel mechanism. We find that BrMT specifically slows early voltage-dependent activation transitions, and a model is proposed for the mechanism by which BrMT slows these activation steps. This work identifies BrMT as a novel reagent that selectively stabilizes Shaker's voltage sensors in their resting conformation.

MATERIALS AND METHODS

BrMT Solutions

BrMT was purified from hypobranchial glands of *Calliostoma canaliculatum* as described previously (Kelley et al., 2003). All concentrations of BrMT cited refer to the active dimeric form. BrMT was diluted from an aqueous stock solution containing residual acetonitrile and trifluoroacetic acid from the purification process. These solvents had no significant effect on channel properties at the dilutions used to study BrMT. BrMT-containing solutions were frozen for long-term storage at −80°C.

BrMT appeared to be light sensitive. After several days of exposure to fluorescent laboratory lighting, degradation was apparent in the UV/visible absorbance spectrum of BrMT solutions. The intensity of the UV/visible absorbance spectrum of BrMT in physiological salt solutions decreased after contact with many different surfaces, suggesting that BrMT was being retained. Materials that appeared to retain BrMT included: polyethylene, polypropylene, polycarbonate, glass, and quartz. The amount of BrMT that a piece of plastic or glassware could retain appeared saturable. To prevent loss of BrMT from solutions, polytetrafluoroethylene (PTFE; Teflon®) was used whenever practical.

Channel Expression

Oocytes. *Xenopus laevis* oocytes were surgically removed, defolliculated with collagenase, and stored at 17°C in ND96 solution (in mM): 96 NaCl, 2 KCl, 1.8 $CaCl_2$, 2 $MgCl_2$, 5 HEPES (pH 7.6) plus 10 μg/ml gentamycin. The *Drosophila* ShakerBΔ6–46 (ShBΔ) constructs had NH_2-terminal residues 6–46 deleted to eliminate fast, N-type inactivation (Hoshi et al., 1990). Unless noted otherwise, a ShBΔ construct with C-type inactivation minimized by the T449Y mutation (Lopez-Barneo et al., 1993) was used to study the effects of BrMT on activation with minimal interference from channel inactivation. The ILT construct (ShBΔ V369I;I372L; S376T) (Smith-Maxwell et al., 1998b) retained a threonine at position 449. The full coding regions of all constructs were verified by nucleotide sequencing. K channel RNA was transcribed with the mMessage Machine® T7 kit (Ambion) following the manufacturer's protocols, and oocytes were injected with RNA 2–7 d before recording.

Mammalian cells. The ShBΔ channel expressed in CHO-K1 cells (American Type Culture Collection) contained the additional mutations C301S, C308S and T449V (Holmgren et al., 1996) and was a gift of G. Yellen, Harvard University. The effects of BrMT on these channels in CHO cells were similar to ShBΔ expressed in oocytes. Cells were plated onto untreated glass coverslips and transfected using calcium phosphate as described elsewhere (Brock et al., 2001). Recordings were performed 1–4 d posttransfection.

Electrophysiology

Macroscopic currents. Excised oocyte patch recordings were made at 22°C in the outside-out or inside-out configuration (Hamill et al., 1981) using an Axopatch 200A or Axopatch 1-B amplifier (Axon Instruments, Inc.). Data were acquired with a ITC-16 interface (Instrutech) on a Macintosh computer (Apple) running Pulse acquisition software (HEKA Electronik). The stimulus pulse was sometimes filtered at 20 kHz to minimize fast capacitance transients. Records were filtered at 10 kHz and digitized at 50 kHz. Most traces shown were digitally smoothed with a 2 kHz Gaussian filter. P/−n leak subtraction was used. Holding potential was −80 mV unless otherwise mentioned.

The external solution for I_K recordings contained (in mM): 115 NaCl, 10 KCl, 2 $MgCl_2$, 2 $CaCl_2$, 20 HEPES (pH 7.2 with HCl). The internal solution contained (in mM): 50 KF, 60 KCl, 30 KOH, 10 EGTA, 20 HEPES (pH 7.2 with HCl). Pipette tip resistances with these solutions were <3 MΩ. In some outside-out patches, effects similar to internal application of BrMT would slowly develop after minutes of exposure to BrMT. To prevent this apparent accumulation of dimeric BrMT in the patch pipette, 2 mM tris-carboxyethylphosphine (TCEP) was added to the internal solution (see Fig. 1). Solution pH was then returned to 7.2 with N-methyl-D-glucamine (NMG). Aliquots of this internal solution were frozen at −20°C until use.

Solutions were applied to patches in a continuous stream using a delivery manifold with a 100 μm diameter port (DAD-12; ALA Scientific Instruments) and a back pressure of 150–300 mm Hg. Solution accessibility was verified for every patch by tetraethylammonium block of I_K.

Single-channel currents. Single-channel recordings were made from outside-out oocyte patches. Unless mentioned otherwise, methods were as described for macroscopic currents. An Axopatch 200A amplifier was used in capacitive feedback mode, and data were initially filtered at 5 kHz. Pipette tip resistances were 3–10 MΩ. All analysis was performed on steps from −100 to +40 mV in the presence or absence of 5 μM external BrMT. Traces were leak subtracted using a partial average of blank sweeps compiled with the Patch Machine program (available at http://

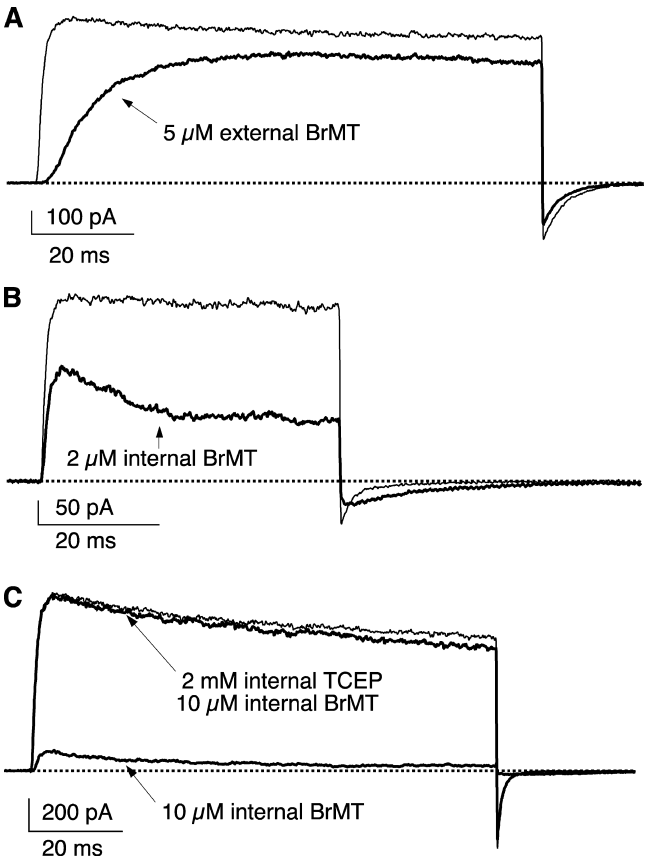

FIGURE 1. Sidedness of BrMT effect on ShBΔ I_K from excised oocyte patches. I_K in A and B is from ShBΔ with C-type inactivation minimized by the T449Y mutation. The ShBΔ channels in C do not contain the mutation at position 449. (A) Effects of external BrMT on ShBΔ I_K from an outside-out patch. BrMT greatly slows activation kinetics and leads to a reduction in peak amplitude. Voltage step to +20 mV from −100 mV. Thin trace: control condition. Thick trace: external solution with 5 μM BrMT. TCEP was not included in the internal solution. (B) BrMT applied to inside-out patches has no apparent effect on activation but reduces peak I_K, induces a decline in amplitude after the peak, and slows deactivation kinetics. Step to +40 mV from −100 mV. Thin trace: control condition. Thick trace: internal solution with 2 μM BrMT. (C) The monomeric form of BrMT does not block ShBΔ channels from the internal side of an inside-out patch. Including the disulfide reducing agent TCEP (2 mM) with 10 μM BrMT eliminates effects of internal BrMT. Voltage step from −80 to +20 mV returning to −120 mV. Thin trace: control condition. Thick traces: internal solution includes either 10 μM BrMT and 2 mM TCEP or 10 μM BrMT but no TCEP.

www.hoshi.org). A typical leak trace spliced the first 0.5–1 ms of the capacitive transient from the average of 10 or more blank sweeps with the sum of multiple exponentials fit to the remainder of the sweep. Data were digitally smoothed at 2 kHz for analysis and display. Idealization of single-channel activity was performed with the TAC analysis package (Bruxton). Transitions between open and closed states were idealized using 50% of the open-channel current as a threshold criterion. Steady-state probability of a channel being open (pOpen) was computed from idealized events from sweeps containing openings, and the first and last events of a sweep were eliminated from this analysis. For open-time analysis, idealization of a sweep was terminated upon the occurrence of substate conductance in the record (Hoshi et al., 1994; Zheng et al., 2001). Mean open times were determined from the square root of logarithmically binned open durations (Sigworth and Sine, 1987). The sweep interval for single-channel experiments was ~200 ms and was partially determined by the processing speed of the acquisition computer. This rapid pulsing rate was not always sufficient for channels to recover from inactivation, and resulted in multiple sequential blank sweeps.

Gating currents. Many unsuccessful attempts were made to measure effects of BrMT on ShBΔ I_g from outside-out oocyte patches, the preparation used for the rest of the experiments in this paper. During application of BrMT, current leak from patches routinely increased, especially at the extreme voltages necessary to perform proper leak subtraction pulses. These leak artifacts induced by BrMT were found to be less severe in mammalian cells patch-clamped in the whole-cell configuration. Effects of BrMT on I_g were therefore recorded from whole CHO-K1 cells transiently expressing ShBΔ.

Unless mentioned otherwise, methods were as described for measuring macroscopic ionic currents. Data were acquired with an Axopatch 200A amplifier, filtered at 10 kHz, and sampled at 50 kHz.

Solutions were chosen to prevent ShBΔ channels from becoming defunct in the absence of permeant ions (Melishchuk et al., 1998). The external (bath) solution contained (in mM): 150 tetraethylammonium chloride, 2 $MgCl_2$, 2 $CaCl_2$, 20 HEPES (pH 7.2). The internal (pipette) solution contained (in mM): 5 CsCl, 86 NMG-Cl, 50 NMG-F, 10 EGTA, 20 HEPES (pH 7.2).

A low-volume (~100 μl) chamber was used for whole-cell recordings. Addition of BrMT was accomplished by flowing a volume >0.5 ml through the chamber. This volume was determined to produce >95% solution exchange as calibrated using tetraethylammonium block of I_K from ShBΔ channels.

Analysis and Graphing

Analysis and graphing were performed with IgorPro software (Wavemetrics), which performs nonlinear least-squares fits using a Levenberg-Marquardt algorithm. All statistics noted are mean ± SE.

Conductance-voltage relations were determined from I_K amplitude at −100 mV after an activating pulse of sufficient duration to maximize I_K. Conductance data were fit using the fourth power of a Boltzmann distribution function:

$$g_K = A\left(\frac{1}{1 + e^{\frac{-(V - V_{1/2})zF}{RT}}}\right)^4. \quad (1)$$

Here A is maximal conductance, z is the number of elementary charges responsive to V, the applied voltage, and $V_{1/2}$ is the voltage at which a single Boltzmann distribution reaches half its maximal value. After fitting with Eq. 1, conductance data f were normalized such that $A = 1$.

RESULTS

Sidedness of BrMT Activity

When applied to the extracellular side of an outside-out patch, 5 μM BrMT greatly slows macroscopic potassium current (I_K) through ShBΔ channels and reduces its peak amplitude (Fig. 1 A). Deactivation kinetics after the activating pulse are unaffected by BrMT.

Fundamentally different effects are seen with application of BrMT to the intracellular side of an inside-out patch (Fig. 1 B). In this case, activation kinetics are not slowed, and I_K declines during the activating pulse. In addition, deactivation is obviously slowed. These effects are characteristic of classic "open-channel block" (Armstrong, 1966) of the type produced by long-chain tetraethylammonium derivatives and mildly hydrophobic amines (see Brock et al., 2001). It appears likely that intracellular BrMT, which contains two amine groups, blocks open K channels in a similar manner. These clear differences between intracellular and extracellular application strongly suggest that BrMT does not rapidly cross the plasma membrane, otherwise both effects should be apparent with bath application to patches of either configuration. BrMT thus appears to have distinct internal and external sites of interaction with ShBΔ channels, and different mechanisms are responsible for modifying I_K in the two cases.

When BrMT's disulfide bond is reduced, external application of the monomeric compound does not slow ShBΔ activation (Kelley et al., 2003). Similarly, monomeric BrMT does not block ShBΔ channels from the internal side (Fig. 1 C).

Throughout the rest of this paper, only effects of externally applied BrMT will be discussed.

Voltage Dependence of BrMT Effects on I_K Activation

The most striking effect of externally applied BrMT is the degree to which it slows K channel activation. BrMT greatly slowed activation of I_K from ShBΔ channels at every voltage tested (Fig. 2 A). In contrast, deactivation kinetics were unaffected by BrMT (Fig. 2 B). As might be expected of a ligand that slows activation transitions, BrMT displaced the midpoint of the g_K-V relation to more positive voltages (Fig. 2 C). In addition, the g_K-V curve appears to saturate at a lower conductance level in BrMT. Thus, K channels are not only slow to open in the presence of BrMT, but a fraction of g_K is eliminated and cannot be recovered by increasing the stimulus potential. After channels were opened in BrMT, the K conductance retained an ohmic instantaneous I_K-V relation similar to control (Fig. 2 D), indicating that reduction of peak I_K in BrMT is not due to a rapid, voltage-dependent block of the ShBΔ conduction path.

To compare the degree of slowing induced by BrMT at different voltages, the final 50% of I_K rise was fit with a single exponential to determine a time constant (τ).

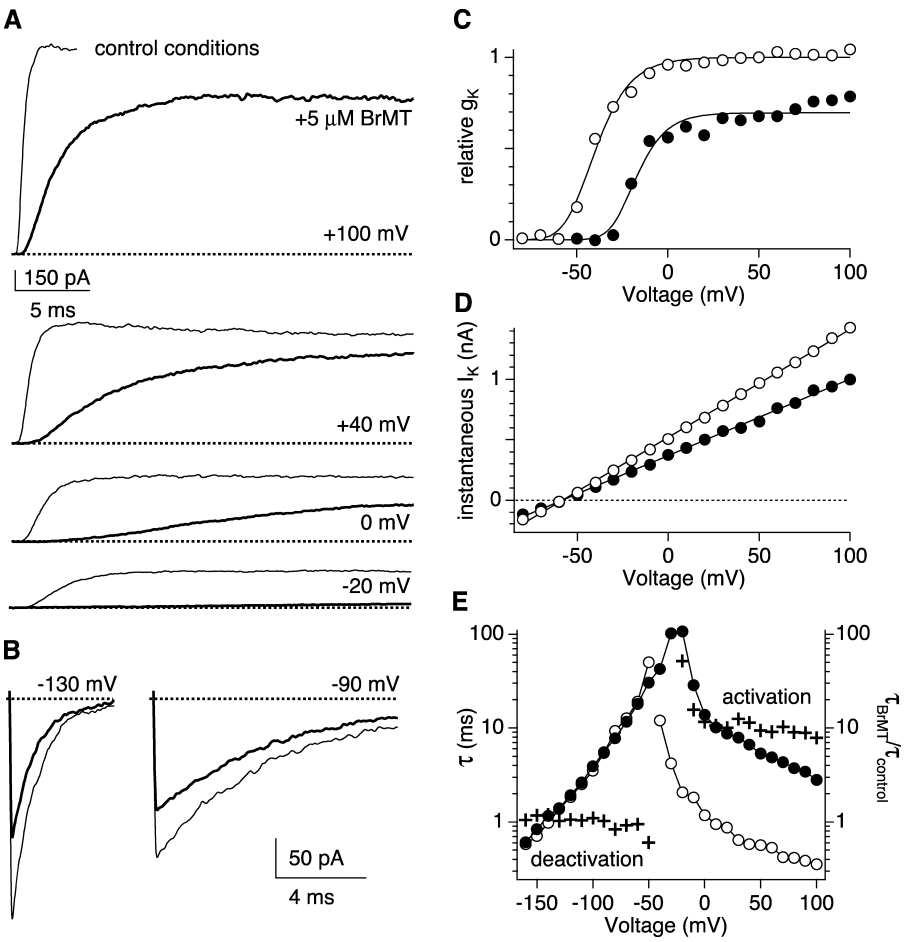

FIGURE 2. Effects of 5 μM BrMT applied externally to ShBΔ channels. Data in all panels are from the same outside-out patch. (A) I_K activation during voltage steps from −100 mV to a series of voltages. Thin traces: control condition. Thick traces: 5 μM BrMT. (B) I_K deactivation after activating pulses to +20 mV. (C) Conductance-voltage relations from tail currents determined in the absence and presence of BrMT. Lines are fits of a fourth-power of a Boltzmann function (control: $V_{1/2} = -59$, $z = 2.1$; 5 μM BrMT: $V_{1/2} = -3.4$, $z = 2.5$). (D) BrMT does not affect rectification or reversal potential. Instantaneous I-V plot was constructed from tail current amplitudes after an activating pulse to +20 mV. Open circles: control condition. Filled circles: 5 μM BrMT. Lines are linear fits to the data. Reversal potentials from these fits are −58.2 mV (control) and −58.1 mV (BrMT). (E) Voltage dependence of activation and deactivation kinetics in the absence and presence of BrMT. Activation time constants were determined by a single exponential fit to the final 50% of the I_K waveform. Deactivation time constants were determined by a single exponential fit to the entire decay of I_K after an activating pulse to +20 mV. Open circles: $\tau_{control}$, control condition. Filled circles: τ_{BrMT}, 5 μM BrMT. Crosses: $\tau_{BrMT}/\tau_{control}$.

The time constant of deactivation after an activating pulse was determined by fitting the entire decay phase of I_K with a single exponential. Activation and deactivation time constants in the absence ($\tau_{control}$) or presence of BrMT (τ_{BrMT}) are compared in Fig. 1 E over a range of voltages. An index of slowing in BrMT is given by $\tau_{BrMT}/\tau_{control}$. Deactivation maintains a $\tau_{BrMT}/\tau_{control}$ ratio of ~1 over all voltages tested, while activation is always slower in BrMT. Activation is uniformly slowed ~10-fold with little voltage-dependence evident between −10 and +100 mV. This is the same voltage range where g_K is largely saturated in BrMT (Fig. 2 C), and hence rates of deactivation transitions are expected to be too slow to affect I_K rise. The similar degree of slowing over this wide voltage range suggests that the intrinsic voltage-sensing of the K channel is responsible for the voltage dependence of ShBΔ activation kinetics in BrMT. A different voltage dependence would be expected if I_K rise in BrMT was a manifestation of voltage-dependent unblock (MacKinnon and Miller, 1988; Goldstein and Miller, 1993).

Concentration Dependence of BrMT

ShBΔ activation is progressively slowed by increasing the concentration of BrMT (Fig. 3 A). At no concentration which induces significant slowing is there any indication of rapidly activating channels that are unaffected by BrMT. Activation slowing (Fig. 3 B) and reduction of I_K amplitude (Fig. 3 C) become notable at a concentration of ~2 μM, and both effects increase smoothly up to 20 μM. As the concentration of BrMT is increased, the midpoint of ShBΔ's g_K-V relation is shifted to increasingly positive voltages (Fig. 3 D). These graded effects on ShBΔ I_K suggest that increasing the concentration of BrMT may slow individual channels in a graded fashion.

Effects of External BrMT on Single K Channels

To better understand the mechanisms of I_K reduction and slowing by BrMT, I_K from single ShBΔ K channels was examined. In 5 μM BrMT, although activation is slowed, single channel I_K appears otherwise similar to the control condition (Fig. 4, A and B). Ensemble averages of sweeps where channels open (Fig. 4 C) demonstrate that BrMT slowing of macroscopic I_K is recapitulated at the single-channel level. In the presence of 5 μM BrMT, time to peak I_K in ensemble averages was ~40 ms (Fig. 4 C), but the cumulative first-latency plot (Fig. 4 D) demonstrates that channels continue to open until somewhat later. This discrepancy is not large, but it suggests that slow inactivation partially obscures the time course of K channel activation in BrMT, even though the ShBΔ channels used for single-channel recordings have inactivation minimized.

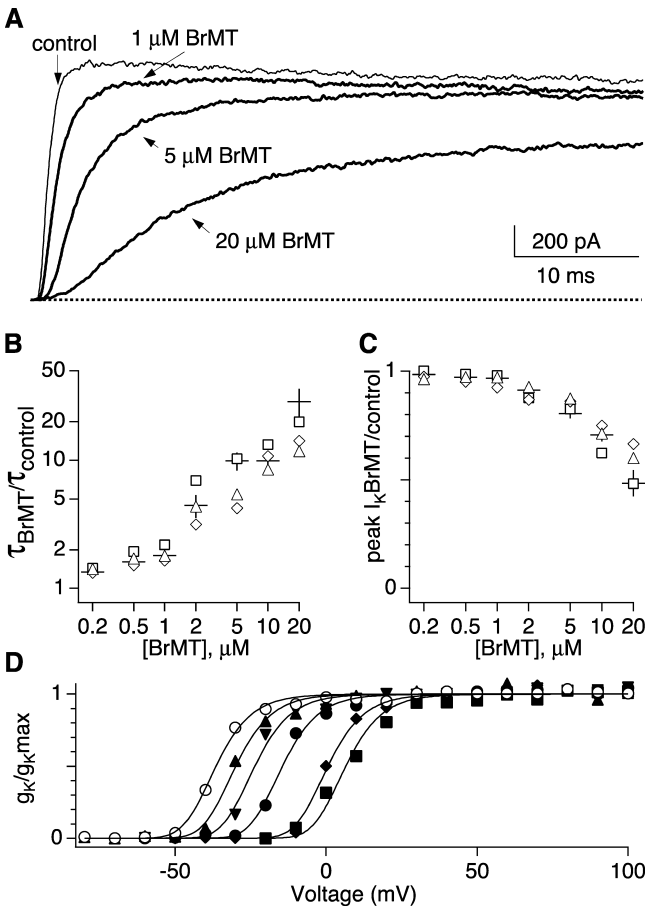

FIGURE 3. Concentration dependence of external BrMT. Dose–response data from outside-out patches containing ShBΔ. (A) Thin trace: ShBΔ I_K in response to a voltage step from −100 to +40 mV. Thick traces: I_K at +40 mV in BrMT. (B) Slowing of I_K activation by BrMT at +40 mV is plotted as the ratio of time constants from fits to activation kinetics ($\tau_{BrMT}/\tau_{control}$). Different symbols represent values from different patches that underwent the entire dose–response. Crosses represent mean ± SE from 4–9 patches. (C) Effect of BrMT on peak I_K amplitude. Peak I_K was measured at +40 mV. Symbols correspond to same patches as in B. Crosses represent mean ± SE from 4–10 patches. (D) Conductance-voltage relations determined from different concentrations of BrMT applied to a single patch. Conductance values are from tail currents at −100 mV. Data at each concentration were normalized to the peak amplitude of a fourth-power Boltzmann fit (lines). Fits to BrMT data were constrained to have the steepness of the fit to control data (z = 3.4). $V_{1/2}$ values from the fourth-power fits: control (open circles) = −49 mV; 1 μM (triangles) = −42 mV; 2 μM (inverted triangles) = −36 mV; 5 μM (filled circles) = −27 mV; 10 μM (diamonds) = −12 mV; 20 μM (squares) = −6 mV.

BrMT slows latency to first opening (Fig. 4, D and H), but after this initial opening ShBΔ behaves similar to control. The unitary conductance in 5 μM BrMT does not change (Fig. 4, E and J) and cannot account for the decrease in peak I_K seen in macroscopic I_K ($P < 0.0001$, Student's *t* test; see Fig. 4 J, legend). The distri-

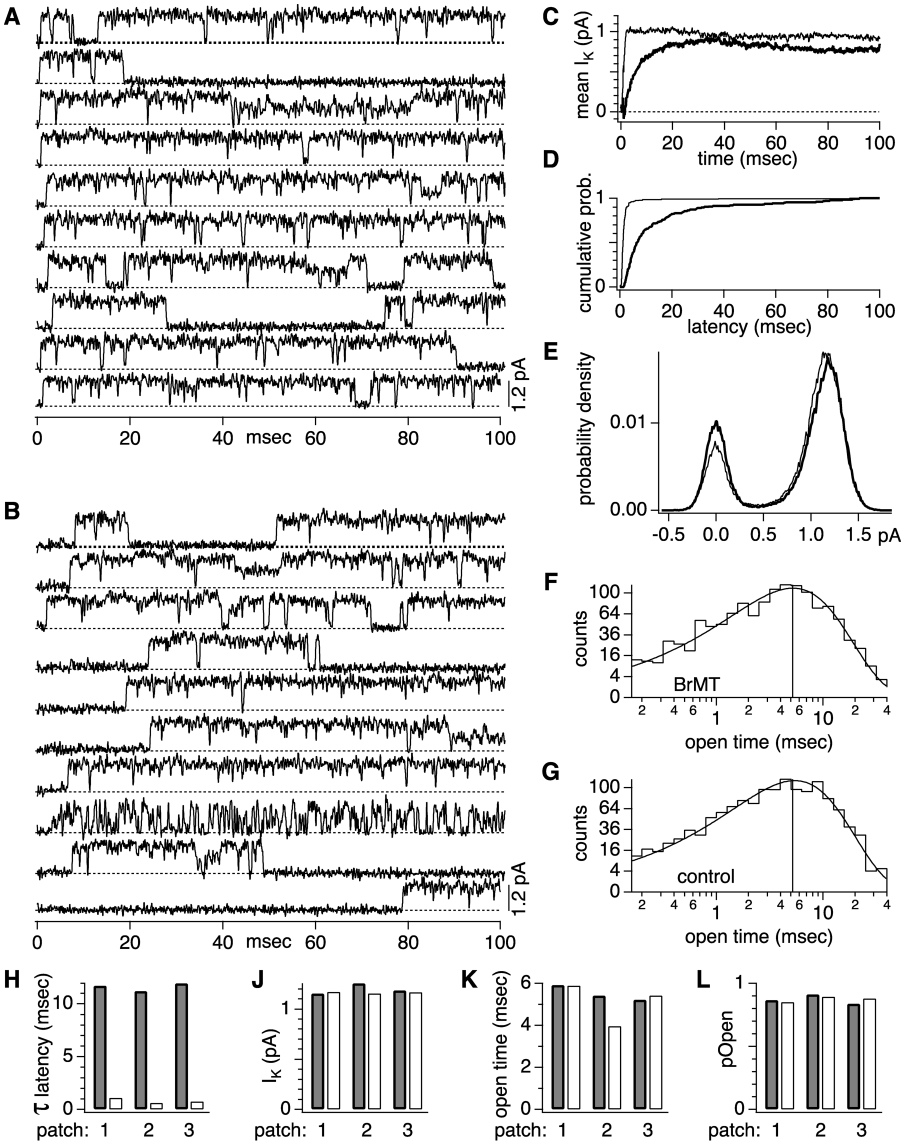

FIGURE 4. Effects of 5 μM BrMT on single ShBΔ channels. Analyses was conducted on I_K from outside-out patches containing one functional ShBΔ channel during 100-ms steps to +40 mV from −100 mV. Data in A–G are from a single patch (patch 3 in H–L). In C–G, analyses of control currents are represented by thin traces, and I_K in 5 μM BrMT by thick traces. In H–L, thick-rimmed grayed bars are measurements in BrMT and hollow bars under control conditions. (A) Representative traces containing single channel openings under control conditions. (B) Openings of the same channel in 5 μM BrMT. (C) Ensemble averages of sweeps containing channel openings (i.e., nonblank sweeps). (D) Cumulative first latencies from sweeps containing openings. (E) Unitary conductance does not change in BrMT. All-points histograms were compiled from sweeps without apparent substates. Bin width is 10 fA. (F) Logarithmically binned open durations in BrMT. Substates were not included in this analysis. Curve is fit for a single open state. The mean open time of 5.2 ms indicated by a vertical line. (G) Open durations under control conditions. Mean open time is 5.4 ms. (H) Time constants of exponential fits to the final 50% rise of cumulative first latencies. (J) Unitary conductance is unchanged by BrMT. Unitary I_K in 5 μM BrMT versus control was 1.01 ± 0.02 (n = 6) while peak macroscopic I_K was reduced to 0.80 ± 0.02 (n = 10). (K) Mean open time is little affected by BrMT (L) Conditional probabilities that a channel is open provided it has opened previously. Calculated for sweeps containing channel openings (see RESULTS and MATERIALS AND METHODS). The first and last idealized events were not included in determination of pOpen.

bution of open times was also little altered by BrMT (Fig. 4, F, G, and K). Likewise, the probability that a channel was open, provided it had opened previously during a voltage step, was unaffected by BrMT (Fig. 4 L). The similar conductance level, mean open time and conditional open probability suggest that BrMT does not affect transitions near the open state.

The single-channel currents indicate that BrMT decreases macroscopic I_K by increasing the probability that a channel will fail to open during a voltage pulse. Under control conditions, 26% of repetitive 100-ms sweeps contained no openings with the rapid pulsing protocol used, whereas in BrMT 51% were blank. These blank sweeps were not included in analyses of single-channel properties. The blanks sweeps tended to occur in long sequential clusters, and are likely due to incomplete recovery from inactivation. This result suggests that BrMT may reduce peak I_K by stabilizing an inactivated state.

Effects of External BrMT on K-channel Gating Current

Actions of BrMT described above point to an inhibitory interaction with the voltage-dependent gating processes underlying activation of ShBΔ channels. These voltage-dependent processes give rise to a gating current (I_g) that is measurable in the absence of conduct-

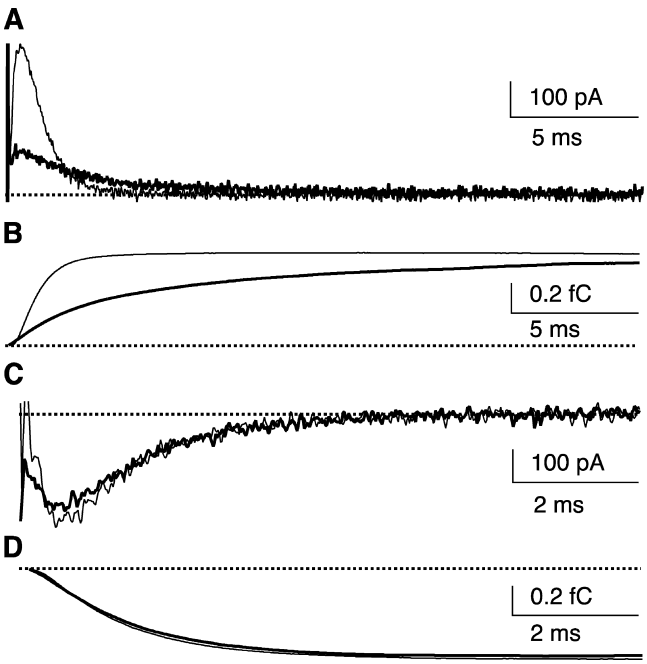

FIGURE 5. Effects of BrMT on ShBΔ gating currents. Gating currents were recorded from CHO-K1 cells expressing ShBΔ channels. Similar effects on ShBΔ I_g were seen in nine cells. Thin traces: control condition. Thick traces: in 5 μM BrMT. The zero current baseline for gating charge integration (Q) was set individually for each trace, after the I_g transient decayed to steady-state. (A) I_gON is slowed and peak amplitude is greatly reduced by BrMT. Voltage steps are to +20 mV from −100 mV. (B) Integrated charge movement (Q_{ON}) from I_gON in A. (C) I_gOFF in BrMT is similar to control. Voltage steps are to −140 mV after a 200-ms activating pulse to +20 mV. (D) Integrated charge movement (Q_{OFF}) from I_gOFF in C. Q_{OFF} in BrMT was 1.02 ± 0.02 that of control, $n = 4$ cells.

ing ions. If BrMT slows voltage-dependent activation transitions then it might also be expected to alter I_g.

ShBΔ gating current during activation (I_gON) was markedly slowed when exposed to 5 μM BrMT (Fig. 5 A). This effect parallels BrMT's slowing of I_K activation, and demonstrates that BrMT inhibits voltage-dependent processes that underlie I_K activation.

In BrMT, a component of I_gON appears to decay very slowly. The integral of this current (Q_{ON}) slowly rises after 10 ms of activating stimulus (Fig. 5 B), but this slow charge movement was difficult to quantitate accurately, as slight displacements from zero greatly affect integration over long time periods. It is likely that some ON charge moves too slowly to be clearly resolved.

I_gOFF during deactivation was little affected by BrMT (Fig. 5 C). In conducting solutions, BrMT reduces the peak level of I_K during an activating pulse (Figs. 1–3). This loss of I_K appears to be due to some channels failing to open during the activating pulse. The conservation of total OFF gating charge (Q_{OFF} in 5 μM BrMT vs. control = 1.02 ± 0.02, $n = 4$ cells, Fig. 5 D) indicates that ShBΔ's gating machinery continues to function in BrMT, even in channels that fail to open. This suggests that the reduction in peak I_K by BrMT is the product of a subpopulation of Shaker channels with functional voltage sensors that are for some reason unavailable for opening during the activating pulse. When ShBΔ is C-type inactivated by the W434F mutation, the channels have apparently normal gating currents, yet fail to open during activating pulses (Yang et al., 1997). Analogously, the reduction of I_K in BrMT may be the result of a stabilized inactivated state from which ShBΔ's gating machinery continues to operate.

ShBΔ ILT Identifies Gating Steps Affected by BrMT

The activation pathway of ShBΔ involves many transitions before channel opening. The slowing of both I_K and I_g indicates that BrMT slows some of these transitions, but these experiments do not clearly define which transitions are affected. The exact number and nature of existing activation transitions are not known. It is clear that a minimum of five activating transitions must occur to account for the sigmoidicity of ShBΔ activation (Zagotta et al., 1994b). The most thorough models of ShBΔ activation require each subunit of the tetrameric channel to undergo at least three transitions before channel opening (Schoppa and Sigworth, 1998c; Ledwell and Aldrich, 1999). It is difficult to identify which of these many transitions are affected by BrMT, because ShBΔ activation transitions occur at overlapping voltage ranges, and a stimulus to any activating voltage will trigger multiple activating transitions.

The ShBΔ gating mutant, V369I;I372L;S376T (ILT) cleanly separates gating steps into distinct voltage ranges (Smith-Maxwell et al., 1998b; Ledwell and Aldrich, 1999). A simple activation scheme depicting differences between "wild-type" ShBΔ and ILT is shown in Fig. 6 A. The ILT mutations shift channel opening to very positive voltages, whereas the majority of activation steps and gating charge movements still occur at negative voltages. When activated from −140 to 0 mV, ShBΔ will traverse all the transitions along its activation path. When activated by the same voltage step, the ILT channel will move most of its gating charge, yet not open. A greater activating potential, e.g., +140 mV, is required to open ILT channels. This separation of activation transitions into distinct voltage ranges allows a test of which transitions are affected by BrMT: early transitions that occur at negative voltages, or the later transitions at positive voltages that allow channel opening.

When ILT channels are stepped from −140 to +140 mV, the full activation pathway is traversed before channel opening. When ILT channels are stepped from 0 to +140 mV, only the later part of the activation path is

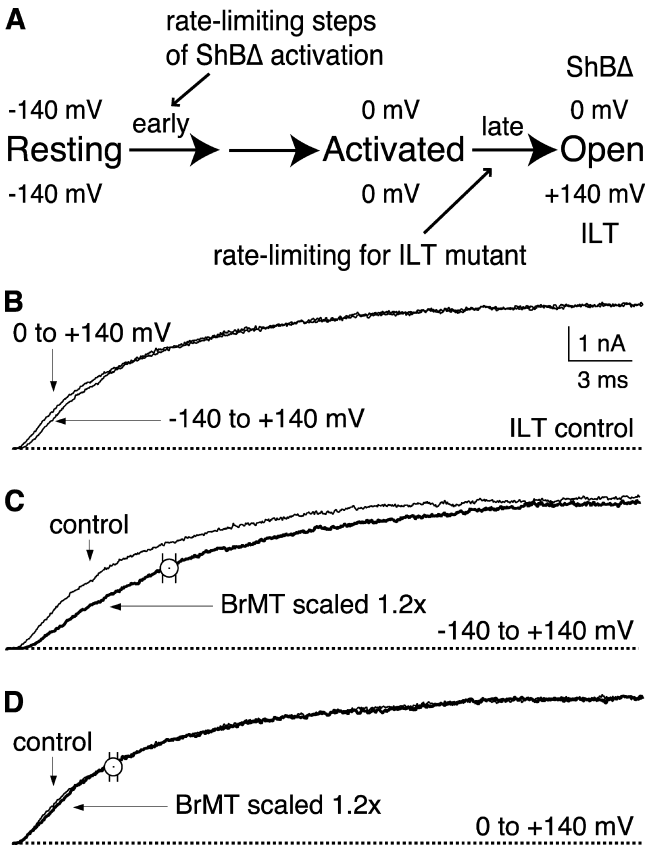

FIGURE 6. BrMT slows early but not late activating transitions of ShBΔ ILT. I_K from ShBΔ V369I;I372L;S376T (ILT) in outside-out patches. HP = −60. Pipette solution did not contain TCEP. (A) Scheme depicting gating of ILT channels. (B) I_K rise from ILT channels at +140 mV after 60-ms prepulses to either −140 or 0 mV. Note the slight delay apparent from −140 mV. (C) ILT activation during a step from −140 mV. I_K in 5 μM BrMT is scaled to match peak control I_K. Open circle: mean time to half maximal I_K in 5 μM BrMT was 1.6 ± 0.2 times that of control, n = 5 patches. (D) ILT activation during a step from 0 mV. I_K in 5 μM BrMT is scaled to match peak control I_K. Note the near perfect I_K overlay indicating that BrMT does not slow the late activation steps of the ILT channel. Open circle: mean time to half maximal I_K in 5 μM BrMT was similar (1.1 ± 0.1 times control, n = 5 patches).

traversed. Under control conditions, channels activate with a similar time course from either prepulse potential (Fig. 6 B). When ILT is activated from −140 mV, BrMT slows I_K activation (Fig. 6 C). When ILT is activated from 0 mV, BrMT has no effect on I_K kinetics (Fig. 6 D), demonstrating that BrMT does not slow steps that occur only above 0 mV in the ILT channel. This lack of a BrMT effect on the final opening step of ILT channels demonstrates that BrMT only inhibits specific transitions early in the activation path. Thus, the effect on ILT activation from −140 mV is due to BrMT slowing early steps such that they become rate limiting for I_K activation. This is consistent with 5 μM BrMT's dramatic slowing of I_K activation and I_gON in "wild-type" ShBΔ.

The specificity of BrMT for early transitions in ILT also demonstrates that late activation transitions are pharmacologically distinguishable from early charge movements. Thus, early and late charge movements must represent distinct classes of conformational transitions.

DISCUSSION

Primary Features of BrMT Action Against ShBΔ Channels

BrMT slows early, but not late activation steps in the ShBΔ activation pathway.

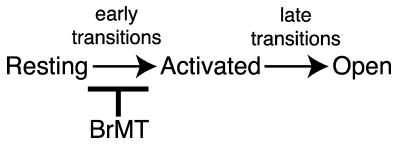

SCHEME I

This activation scheme (Scheme I) is a simplified depiction of more complex published models (Schoppa and Sigworth, 1998c; Ledwell and Aldrich, 1999). The proposition that BrMT slows voltage-dependent steps early in ShBΔ's activation pathway takes into account the following points:

1. BrMT slows I_K activation and does not affect deactivation. Activation kinetics are profoundly slowed by BrMT, and time constants from the slowed I_K rise have the same voltage dependence as control I_K (Fig. 2). This suggests that BrMT slows the early gating steps that are rate limiting for I_K rise under control conditions (Zagotta et al., 1994a; Schoppa and Sigworth, 1998c; Smith-Maxwell et al., 1998b; Ledwell and Aldrich, 1999). The lack of any BrMT effect on I_K deactivation clearly indicates that BrMT does not affect the rate-limiting deactivation transitions near the open state.

2. BrMT slows opening, but once open, single channels behave normally. BrMT lengthens latency to first opening, but does not alter unitary conductance amplitude, mean open time, or steady-state open probability (Fig. 4). This suggests that BrMT stabilizes the channel's closed states, but has little effect on the open state or transitions late in the activation pathway. The rapid, flickery closing transitions near the open state (Hoshi et al., 1994; Schoppa and Sigworth, 1998a) are not altered by BrMT. These findings are all consistent with a mechanism in which BrMT inhibits K channels by stabilizing closed states early in the activation pathway.

3. BrMT selectively slows ON gating charge movement. A large, fast component of I_gON is slowed by BrMT (Fig. 5). This I_gON component represents voltage-sensor movements early in the activation pathway (Zagotta et

al., 1994a; Schoppa and Sigworth, 1998c), and BrMT clearly impedes these steps. After channels have been fully activated, I_gOFF is little affected by BrMT. Failure of BrMT to alter this deactivation-related signal again indicates that BrMT does not greatly affect deactivation transitions.

4. BrMT does not affect the final opening step. BrMT only slows early activation steps of the ShBΔ ILT mutant. When ILT channels open after traversing only late activation steps (Fig. 6), BrMT does not slow I_K activation.

These findings clearly demonstrate that BrMT modifies ShBΔ gating by selectively slowing voltage-sensitive transitions early in the activation pathway. How does BrMT binding slow activation in such a fashion? To address this question, a key feature of BrMT's effect was examined further: the graded slowing of I_K as BrMT concentration is increased.

Rapid Binding of BrMT to Closed Channels Can Account for Graded Activation Slowing

To understand the mechanism by which BrMT slows activation of ShBΔ K channels, two models of activation slowing are tested here. One assumes that BrMT binds and unbinds channels more slowly than they activate, while the other assumes that BrMT is always at a rapid binding equilibrium with K channels.

Slow BrMT Binding

If there is little ligand exchange during activation, binding sites occupied by BrMT would remain occupied during channel activation, and vacant sites remain vacant. A simple model where one BrMT molecule binds a channel and slows its activating transition is depicted in Scheme II.

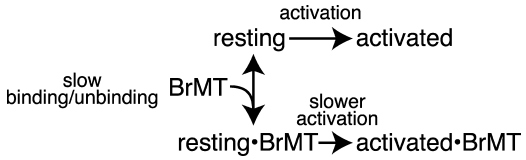

SCHEME II

In this scheme, two populations of channels exist: those with and those without BrMT. Channels without BrMT activate normally, while those bound to BrMT activate more slowly. The equilibrium constant (K_{eq}) determining the ratio of bound versus unbound channels is simply:

$$K_{eq} = \frac{[BrMT]}{K_D} \quad (2)$$

The Shaker channel contains four identical subunits. If we assume BrMT binds independently to each subunit, then the proportion of channels with 0, 1, 2, 3, or 4 BrMT bound at any given time would follow a binomial distribution as depicted in Scheme III.

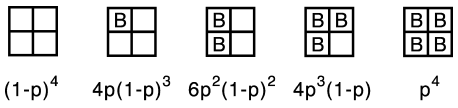

SCHEME III

The most extensive models of ShBΔ activation suggest that early transitions occur independently in each subunit (Zagotta et al., 1994a; Schoppa and Sigworth, 1998c; Ledwell and Aldrich, 1999; Mannuzzu and Isacoff, 2000). When subunits activate independently, they are not affected by the activation state of other subunits. Fig. 7 B demonstrates a model in which BrMT slows activation of each subunit when bound. With such a model, biphasic I_K rise is seen at subsaturating concentrations of BrMT, rather than the graded slowing of activation seen experimentally. This model clearly does not recapitulate the experimentally observed slowing of I_K. Many other attempts were made with related slow-binding models to mimic the effects of BrMT, but no plausible scheme was ever found to produce an appropriately graded slowing of activation.

Rapid BrMT Binding

To construct a model in which BrMT produces a graded slowing of activation, BrMT was assumed to rapidly bind resting channel conformations. If BrMT rapidly binds and unbinds a channel on a time scale faster than activation, then the graded slowing with increasing BrMT concentration can be simply accounted for. Scheme IV depicts BrMT binding only to subunits with voltage sensors in a resting conformation, such that they cannot activate when BrMT is bound:

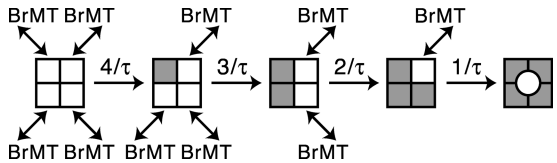

SCHEME IV

A double-headed arrow connecting BrMT to a white subunit indicates that BrMT can rapidly bind a resting subunit and prevent its activation. Grayed subunits have undergone their activating transition, and no longer bind BrMT. The hollowed channel depicts the open state. If BrMT binding is at a rapid equilibrium relative to the rate of voltage-sensor activation, the de-

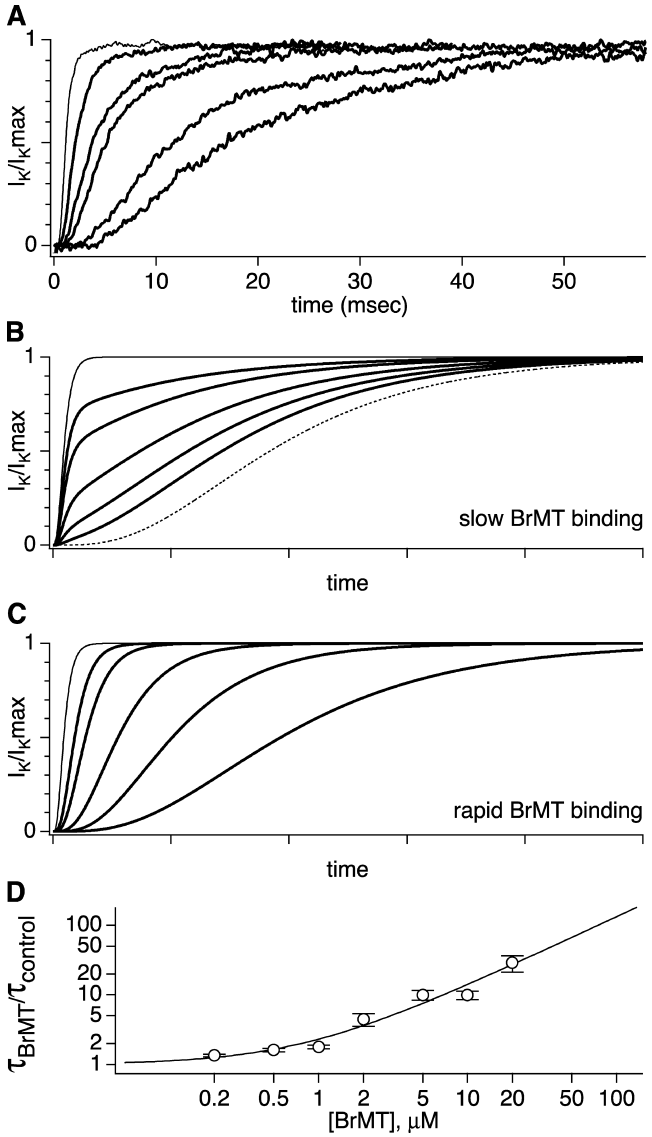

FIGURE 7. Graded activation slowing can be modeled by rapid, reversible binding of BrMT to resting voltage sensors. (A) ShBΔ I_K scaled to match peak current amplitudes. Thin trace: voltage step from −100 to +40 mV under control conditions. Thick traces: progressive slowing of activation at +40 mV by 1, 2, 5, 10, and 20 μM BrMT. (B) Predicted I_K from an activation model with slow BrMT binding to each of four subunits that undergo a single activating transition. Subunits bound to BrMT activate 20-fold slower than those without. This value was chosen because the maximal slowing of ShBΔ activation seen was ~20-fold in BrMT versus control (see D). The proportion of channels with 0, 1, 2, 3, or 4 BrMT bound was binomial. Thin line: control condition. Dotted line: saturating BrMT. Thick lines: [BrMT] = 0.2, 0.5, 1, 2, and 5× K_D. (C) Predicted I_K from Eq. 4. This equation represents an n^4 model of activation with rapid BrMT binding as in Scheme IV. Increasing the concentration of BrMT slows activation by increasing the proportion of time subunits are bound to BrMT and thus unable to activate. Thin line: control condition. Thick lines: [BrMT] = 1, 2, 5, 10, and 20× K_D. (D) Filled circles: ratio of τ_{BrMT} and $\tau_{control}$ at +40 mV, n = 4–9. Line: fit of rapid binding model (Eq. 3) to data. K_D from fit = 0.8 μM.

gree of activation slowing of each subunit in Scheme IV is determined by:

$$\frac{\tau_{BrMT}}{\tau_{control}} = 1 + \frac{[BrMT]}{K_D} \quad (3)$$

This mechanism of slowing is similar to how rapid open channel blockers, such as internal tetraethylammonium, slow I_K deactivation (Armstrong, 1966, 1971; Choi et al., 1993). In this scheme, activation slowing is proportional to the probability that BrMT is bound. As the concentration of BrMT is increased above its K_D, activation of each subunit becomes slower because it is bound to BrMT a greater proportion of the time. If each subunit of a homotetrameric channel activates independently, then this activation model is analytically described by the fourth power of an exponential rise in which the underlying time constant of activation is determined by Eq. 3:

$$I_K = A\left(1 - e^{\frac{-t}{(1+[BrMT]/K_D)\tau}}\right)^4 \quad (4)$$

I_K predicted by Eq. 4 produces a graded slowing of activation and increases the delay before I_K rise (Fig. 7 C). The striking similarity between this model and I_K activation in BrMT (Fig. 7 A) suggests that BrMT slows activation by rapidly binding and stabilizing resting voltage sensor conformations. The degree of slowing predicted by Eqs. 3 and 4 fits the slowing seen experimentally (Fig. 7 D), further implicating this fast-binding mechanism in BrMT's slowing of ShBΔ I_K.

One potential inconsistency with this mechanistic proposal is the slow wash-out of BrMT seen experimentally. While ShBΔ channels activate on a millisecond time scale, the effects of BrMT require many seconds to completely wash-in or wash-out (unpublished data). Although this might indicate that BrMT binds and unbinds on a time scale much slower than channel activation, we suggest the wash-out kinetics of BrMT are unrelated to the microscopic rate of BrMT unbinding from the channel. The kinetics of BrMT wash-in and wash-out were highly variable, and wash-out from outside-out patches was often incomplete after minutes in BrMT-free solutions. Wash-in kinetics of the BrMT effect on ShBΔ I_K in mammalian cells or whole oocytes were even more variable and complete wash-out was rarely obtained in these preparations. The variable kinetics of wash-in and wash-out are likely due to a complex process dependent on solution flow and membrane topology rather than the microscopic binding rate of BrMT to K channels. This may reflect an accumulation of BrMT in or around the plasma membrane. The greasy aromatic rings of BrMT may aggregate with lipids and other hydrophobic molecules. BrMT has a propensity to stick to plasticware (see MATERIALS AND METHODS) and is strongly retained by hydrophobic col-

umns during reverse phase HPLC (Kelley et al., 2003), indicating that BrMT is not highly soluble in aqueous solution. Also, some form of accumulation of BrMT could explain the tendency for micromolar concentrations of BrMT to disrupt the patch clamp seal.

If BrMT accumulates in or around membranes, the local concentration of BrMT around K channels would be different from that in the external solution. Thus, the apparent K_D of 0.8 μM (Fig. 7 D) refers to the concentration of BrMT in aqueous solution and not to the presumably higher local concentration surrounding the channels. ShBΔ's actual K_D for BrMT is therefore difficult to determine.

Similarity to Divalent Cations?

Activation of Kv1 family channels, including squid delayed rectifier (Gilly and Armstrong, 1982), Shaker B (Spires and Begenisich, 1994), and hKv1.5 (Zhang et al., 2001) channels, are inhibited by zinc and other divalent transition metal ions in a way that resembles the action of BrMT. Specifically, activation kinetics are slowed, but deactivation kinetics are affected to a much lesser extent. A key feature of the action of both BrMT and zinc ions is the selective and smoothly graded slowing of I_K activation kinetics with little evidence for a population of unmodified channels at intermediate ligand concentrations (compare Fig. 3 A with Fig. 2 A of Gilly and Armstrong, 1982). In both cases the dramatic I_K slowing is essentially voltage independent and the g_K-V relationship is only modestly shifted.

Extracellular magnesium and other divalent ions also slow activation of EAG K channels. Magnesium induces a change in EAG I_K that is qualitatively different from the effects of BrMT or divalent transition metals on Kv channels. The relative amplitudes of fast and slow components of EAG I_K vary with magnesium concentration. However, the effect of magnesium on EAG appears mechanistically similar to the effect of BrMT on ShBΔ. Magnesium induces a graded slowing of early EAG activation steps, slows I_gON, has no apparent effect on later activation steps, and no effect on deactivation (Terlau et al., 1996; Tang et al., 2000). Terlau and coworkers propose a model of activation slowing whereby magnesium stabilizes resting voltage-sensor conformations from which EAG is slow to activate. As the concentration of magnesium increases, more voltage sensors occupy this stabilized resting state. The biggest difference between the Terlau et al. (1996) magnesium versus EAG model and our BrMT versus ShBΔ model is that BrMT stabilizes a state already occupied at rest in the absence of BrMT.

The coupling of divalent ion binding to the graded slowing of I_K activation has never been fully understood. As the effects of divalent ions are very similar to those of BrMT, a reinterpretation of their inhibitory effects using a rapid-binding model may prove fruitful.

Usefulness of BrMT

Here we show BrMT to be a unique gating modifier that inhibits specific gating steps early in a K channel's activation pathway. BrMT acts by slowing the early activation steps. Other activation steps, which influence the time course of I_K activation under control conditions, are rendered insignificant or "silent" because they occur much more quickly than the BrMT-slowed steps. Thus, BrMT can slow I_K activation until its time course is determined almost solely by these BrMT-slowed steps. This allows the BrMT-sensitive steps to be more carefully studied. The ILT mutations, which specifically slow the final opening of Shaker channels, have been used to determine the voltage dependence and cooperativity among subunits during channel opening (Smith-Maxwell et al., 1998a,b; Ledwell and Aldrich, 1999). BrMT retards early voltage-sensor movements, and it can be used in an analogous fashion to study early gating steps. Work is currently ongoing to define biophysical properties of the early, BrMT-sensitive steps in Shaker's activation path.

We thank Wayne Kelley and the laboratory of Jonathan Sweedler (U. Illinois Urbana-Champaign) for purified BrMT.

J.T. Sack was supported by a National Institutes of Health training grant to Stanford University, a grant from Myers Oceanographic and Marine Biology Trust, a predoctoral fellowship from the American Heart Association Western States Affiliate, and the Howard Hughes Medical Institute. R.W. Aldrich is an investigator with the Howard Hughes Medical Institute. This work was supported by National Institutes of Health grant NS-17510 (W.F. Gilly).

David C. Gadsby served as editor.

Submitted: 24 February 2004
Accepted: 12 April 2004

REFERENCES

Armstrong, C.M. 1966. Time course of TEA^+-induced anomalous rectification in squid giant axons. *J. Gen. Physiol.* 50:491–503.

Armstrong, C.M. 1971. Interaction of tetraethylammonium ion derivatives with the potassium channels of giant axons. *J. Gen. Physiol.* 58:413–437.

Armstrong, C.M., and A. Loboda. 2001. A model for 4-aminopyridine action on k channels: similarities to tetraethylammonium ion action. *Biophys. J.* 81:895–904.

Baker, O.S., H.P. Larsson, L.M. Mannuzzu, and E.Y. Isacoff. 1998. Three transmembrane conformations and sequence-dependent displacement of the S4 domain in shaker K^+ channel gating. *Neuron.* 20:1283–1294.

Bezanilla, F., E. Perozo, and E. Stefani. 1994. Gating of Shaker K^+ channels: II. The components of gating currents and a model of channel activation. *Biophys. J.* 66:1011–1021.

Brock, M.W., C. Mathes, and W.F. Gilly. 2001. Selective open-channel block of Shaker (Kv1) potassium channels by s-nitrosodithiothreitol (SNDTT). *J. Gen. Physiol.* 118:113–134.

Choi, K.L., C. Mossman, J. Aube, and G. Yellen. 1993. The internal

quaternary ammonium receptor site of Shaker potassium channels. *Neuron.* 10:533–541.

Gilly, W.F., and C.M. Armstrong. 1982. Divalent cations and the activation kinetics of potassium channels in squid giant axons. *J. Gen. Physiol.* 79:965–996.

Goldstein, S.A., and C. Miller. 1993. Mechanism of charybdotoxin block of a voltage-gated K^+ channel. *Biophys. J.* 65:1613–1619.

Hamill, O.P., A. Marty, E. Neher, B. Sakmann, and F.J. Sigworth. 1981. Improved patch-clamp techniques for high-resolution current recording from cells and cell-free membrane patches. *Pflugers Arch.* 391:85–100.

Holmgren, M., M.E. Jurman, and G. Yellen. 1996. N-type inactivation and the S4-S5 region of the Shaker K^+ channel. *J. Gen. Physiol.* 108:195–206.

Holmgren, M., P.L. Smith, and G. Yellen. 1997. Trapping of organic blockers by closing of voltage-dependent K^+ channels: evidence for a trap door mechanism of activation gating. *J. Gen. Physiol.* 109:527–535.

Hoshi, T., W.N. Zagotta, and R.W. Aldrich. 1990. Biophysical and molecular mechanisms of Shaker potassium channel inactivation. *Science.* 250:533–538.

Hoshi, T., W.N. Zagotta, and R.W. Aldrich. 1994. Shaker potassium channel gating. I: Transitions near the open state. *J. Gen. Physiol.* 103:249–278.

Kelley, W.P., A.M. Wolters, J.T. Sack, R.A. Jockusch, J.C. Jurchen, E.R. Williams, J.V. Sweedler, and W.F. Gilly. 2003. Characterization of a novel gastropod toxin (6-bromo-2-mercaptotryptamine) that inhibits shaker K channel activity. *J. Biol. Chem.* 278:34934–34942.

Ledwell, J.L., and R.W. Aldrich. 1999. Mutations in the S4 region isolate the final voltage-dependent cooperative step in potassium channel activation. *J. Gen. Physiol.* 113:389–414.

Loboda, A., and C.M. Armstrong. 2001. Resolving the gating charge movement associated with late transitions in K channel activation. *Biophys. J.* 81:905–916.

Lopez-Barneo, J., T. Hoshi, S.H. Heinemann, and R.W. Aldrich. 1993. Effects of external cations and mutations in the pore region on C-type inactivation of Shaker potassium channels. *Receptors Channels.* 1:61–71.

MacKinnon, R., and C. Miller. 1988. Mechanism of charybdotoxin block of the high-conductance, Ca^{2+}-activated K^+ channel. *J. Gen. Physiol.* 91:335–349.

Mannuzzu, L.M., and E.Y. Isacoff. 2000. Independence and cooperativity in rearrangements of a potassium channel voltage sensor revealed by single subunit fluorescence. *J. Gen. Physiol.* 115:257–268.

Melishchuk, A., and C.M. Armstrong. 2001. Mechanism underlying slow kinetics of the OFF gating current in Shaker potassium channel. *Biophys. J.* 80:2167–2175.

Melishchuk, A., A. Loboda, and C.M. Armstrong. 1998. Loss of shaker K channel conductance in 0 K^+ solutions: role of the voltage sensor. *Biophys. J.* 75:1828–1835.

Schoppa, N.E., and F.J. Sigworth. 1998a. Activation of shaker potassium channels. I. Characterization of voltage-dependent transitions. *J. Gen. Physiol.* 111:271–294.

Schoppa, N.E., and F.J. Sigworth. 1998b. Activation of Shaker potassium channels. II. Kinetics of the V2 mutant channel. *J. Gen. Physiol.* 111:295–311.

Schoppa, N.E., and F.J. Sigworth. 1998c. Activation of Shaker potassium channels. III. An activation gating model for wild-type and V2 mutant channels. *J. Gen. Physiol.* 111:313–342.

Sigworth, F.J., and S.M. Sine. 1987. Data transformations for improved display and fitting of single-channel dwell time histograms. *Biophys. J.* 52:1047–1054.

Smith-Maxwell, C.J., J.L. Ledwell, and R.W. Aldrich. 1998a. Role of the S4 in cooperativity of voltage-dependent potassium channel activation. *J. Gen. Physiol.* 111:399–420.

Smith-Maxwell, C.J., J.L. Ledwell, and R.W. Aldrich. 1998b. Uncharged S4 residues and cooperativity in voltage-dependent potassium channel activation. *J. Gen. Physiol.* 111:421–439.

Spires, S., and T. Begenisich. 1994. Modulation of potassium channel gating by external divalent cations. *J. Gen. Physiol.* 104:675–692.

Tang, C.Y., F. Bezanilla, and D.M. Papazian. 2000. Extracellular Mg^{2+} modulates slow gating transitions and the opening of *Drosophila ether-a-Go-Go* potassium channels. *J. Gen. Physiol.* 115:319–338.

Terlau, H., J. Ludwig, R. Steffan, O. Pongs, W. Stuhmer, and S.H. Heinemann. 1996. Extracellular Mg^{2+} regulates activation of rat eag potassium channel. *Pflugers Arch.* 432:301–312.

Yang, Y., Y. Yan, and F.J. Sigworth. 1997. How does the W434F mutation block current in Shaker potassium channels? *J. Gen. Physiol.* 109:779–789.

Zagotta, W.N., T. Hoshi, and R.W. Aldrich. 1994a. Shaker potassium channel gating. III: Evaluation of kinetic models for activation. *J. Gen. Physiol.* 103:321–362.

Zagotta, W.N., T. Hoshi, J. Dittman, and R.W. Aldrich. 1994b. Shaker potassium channel gating. II: Transitions in the activation pathway. *J. Gen. Physiol.* 103:279–319.

Zhang, S., S.J. Kehl, and D. Fedida. 2001. Modulation of Kv1.5 potassium channel gating by extracellular zinc. *Biophys. J.* 81:125–136.

Zheng, J., L. Vankataramanan, and F.J. Sigworth. 2001. Hidden Markov model analysis of intermediate gating steps associated with the pore gate of shaker potassium channels. *J. Gen. Physiol.* 118:547–564.